

# Assessing accuracy of CFD simulations through quantification of a numerical dissipation rate

G. Sun, J.A. Domaradzki, X. Xiang

Department of Aerospace and Mechanical Engineering  
University of Southern California  
Los Angeles, California 90089-1191  
guangrus@usc.edu, jad@usc.edu, xinjianx@usc.edu

K. K. Chen

Institute for Defense Analyses  
Center for Communications Research - La Jolla  
San Diego, CA 92121-1969  
kkchen@ccrwest.org

## ABSTRACT

The accuracy of CFD simulations is typically assessed through a time consuming process of multiple runs and comparisons with available benchmark data. We propose a new method that is both more efficient and general and which allows to assess the accuracy of CFD simulations in the course of actual runs. The method is based on the numerical dissipation analysis proposed by Schraner *et al.* (2015) which allows to compute the numerical dissipation rate and the numerical viscosity for arbitrary sub-domains at each time step in a simulation. As a criterion for accurate simulations we use the requirements that the numerical dissipation should be less than 1% of the physical, viscous dissipation. A simulation initiated on a coarse mesh is run for a short time interval, the numerical dissipation computed, and if the criterion is not satisfied the mesh is refined. This adaptive mesh refinement process is repeated until the criterion is satisfied and the final refined mesh is then used to generate physically accurate simulation results. In principle the method can be applied to an arbitrary Navier-Stokes solver, compressible or incompressible, and structured or unstructured mesh. In this paper we demonstrate the utility of the proposed approach through a series of simulations for a weakly turbulent wake past a sphere at  $Re = 1000$  performed using the OpenFOAM solver.

## INTRODUCTION

The accuracy of numerical simulations of fluid flows is always affected by truncation errors introduced by discretization of governing equations. These errors can only be neglected in Direct Numerical Simulations (DNS) using well resolved time step and mesh size. In principle results of simulations with inadequate resolution, e.g., with the mesh size much larger than the Kolmogoroff length scale, should be physically inaccurate because of the presence of significant truncation errors. However, it is well known that in practice under-resolved DNS (UDNS) are capable of producing surprisingly accurate results for many quantities of interest (e.g., the pressure and friction coefficients for simple airfoils (Castiglioni & Domaradzki, 2015a)). Such UDNS are sometimes known as implicit Large Eddy Simulations (ILES) and are justified by claiming that the dissipative effects of the truncation error are similar to the effects of explicit Subgrid Scale (SGS) models. To quantitatively assess this claim one needs to know the value of the numerical dissipation associated with the truncation errors in a given run. This need provided an incentive to develop techniques to compute the numerical dissipation. The method to quantify numerical dissipation rate was first proposed by Domaradzki *et al.* (2003) and Domaradzki & Radhakrishnan (2005) in the context of the spectral eddy viscosity. That method required the use of an auxiliary spectral code, complicating its application to general Navier-Stokes solvers. More recently, the approach evolved allowing the estimation of the numerical dissipation rate and the numerical viscosity entirely in the physical space representation (Schraner *et al.*, 2015). The method was first tested for a three-dimensional Taylor-Green vortex flow simula-

ted on a structured, Cartesian mesh using a finite volume code. The procedure was subsequently applied by Castiglioni & Domaradzki (2015a) to a realistic flow configuration (a laminar separation bubble flow over a NACA 0012 airfoil at  $Ma = 0.4$  and  $Re = 50,000$ ) simulated on an unstructured mesh using a commercial code.

While the method to quantify the numerical dissipation was originally developed in the context of ILES it has a potential to improve the DNS methodology as well because the numerical dissipation is a measure of the truncation errors. This work provides an example such an application where the method has been applied to analyze and improve numerical simulation results obtained using OpenFOAM software for a flow around a sphere at Reynolds number of 1000. We were motivated by an observation that the Strouhal number in the simulations depended on the resolution used and there was no simple way of estimating the accuracy of the results but through a time consuming and computationally expensive process of performing several runs with increasing resolution until the Strouhal number matched the benchmark data (Kim & Durbin, 1988; Tomboulides & Orszag, 2000; Orr *et al.*, 2015). However, since the numerical dissipation serves as an estimate of numerical errors its knowledge can be used to determine the accuracy of the simulations and circumvent the costly trial and error validation process. This paper describes how this is done.

## BASIC EQUATIONS

The governing equation of fluid flow are the Navier-Stokes equations, for incompressible flow and Newtonian fluid in present work

$$\frac{\partial u_i}{\partial t} + u_j \frac{\partial u_i}{\partial x_j} = -\frac{1}{\rho} \frac{\partial p}{\partial x_i} + \nu \frac{\partial^2 u_i}{\partial x_j^2} \quad (1)$$

where  $u_i$  are the components of the velocity vector,  $\rho$  is the density,  $p$  is the pressure, and  $\nu$  is the kinematic viscosity

## Numerical Dissipation and Viscosity

For turbulent flow, the transport equation of the kinetic energy ( $e_{kin} = \frac{1}{2} u_i u_i$ ) is

$$\frac{\partial \rho e_{kin}}{\partial t} + \frac{\partial (\rho e_{kin} u_i)}{\partial x_i} = -u_i \frac{\partial p}{\partial x_i} + \mu u_j \frac{\partial \tau_{ij}}{\partial x_i} \quad (2)$$

where  $\mu = \rho \nu$  is the dynamic viscosity and  $\tau_{ij}$  is the stress tensor.

For incompressible flow,  $\nabla \cdot \vec{u} = \frac{\partial u_i}{\partial x_i} = 0$ , and the above equation becomes

$$\frac{\partial e_{kin}}{\partial t} + \frac{\partial (e_{kin} u_i)}{\partial x_i} + \frac{1}{\rho} \frac{\partial (p u_i)}{\partial x_i} - \nu \frac{\partial (u_j \tau_{ij})}{\partial x_i} + \nu \tau_{ij} \frac{\partial u_j}{\partial x_i} = 0, \quad (3)$$

For a Newtonian fluid, the kinetic energy equation can be re-written as

$$\frac{\partial e_{kin}}{\partial t} + \frac{\partial(e_{kin}u_i)}{\partial x_i} + \frac{1}{\rho} \frac{\partial(pu_i)}{\partial x_i} - \frac{\partial}{\partial x_i} \left( \nu \frac{\partial e_{kin}}{\partial x_i} \right) + \nu \frac{\partial u_j}{\partial x_i} \frac{\partial u_j}{\partial x_i} = 0. \quad (4)$$

Following the procedure described by Schraner *et al.* (2015) and Castiglioni & Domaradzki (2015a) the discretized terms in the above equation for a computational cell are obtained by computing the time derivative by central differences and the remaining terms using the discretized variables obtained from the solver. Often, the entire equation is integrated over a selected sub-domain consisting of several individual cells. In CFD simulations a numerical Navier-Stokes solver enforces discretized momentum equation on a given mesh. However, the kinetic energy equation is a derived equation that is not solved directly by a solver. As a result, the terms in the discretized energy equation do not sum to zero, leaving a nonvanishing residual

$$\frac{E_{kin}^{n+1} - E_{kin}^{n-1}}{2\Delta t} + F_{kin} + F_{ac} - F_{vis} + \varepsilon_{vis} = -\varepsilon_n, \quad (5)$$

where the terms on the l.h.s correspond to respective terms on the l.h.s of equation (4):  $E_{kin}$  is the kinetic energy in a sub-domain,  $F_{kin}$ ,  $F_{ac}$  and  $F_{vis}$  are contributions from the advective, pressure, and viscous fluxes, respectively, and  $\varepsilon_{vis}$  is the integral form of the viscous (or physical) dissipation.

The residual  $\varepsilon_n$  is called the numerical dissipation rate because it has a predominantly dissipative character if integrated over a sufficiently large control volume.

### Effective Viscosity and Reynolds Number

Comparing the numerical dissipation with the viscous dissipation for a given sub-domain, allows to define the numerical viscosity for that sub-domain as

$$\nu_n = \nu \frac{\varepsilon_n}{\varepsilon_{vis}}. \quad (6)$$

In numerical simulations the effective viscosity is a sum of the physical viscosity  $\nu$  (a nominal value used in the code) and the numerical viscosity  $\nu_n$  due to the numerical dissipation. This allows to define the effective Reynolds number in terms of the nominal Reynolds number

$$Re_{eff} = \frac{UL}{\nu_{eff}} = \frac{UL}{\nu} \frac{\nu}{\nu + \nu_n} = Re \frac{\nu}{\nu + \nu_n} = \frac{Re}{1 + \nu_n/\nu} = \frac{Re}{1 + \varepsilon_n/\varepsilon_{vis}}, \quad (7)$$

where  $U$  is free-stream velocity and  $L$  is characteristic length scale.

## RESULTS

In the present work, the analysis of the numerical dissipation rate and viscosity is applied to a series of UDNS runs for a flow around a sphere at the nominal Reynolds number  $Re = UD/\nu = 1000$  based on the free stream velocity  $U$  and the sphere diameter  $D$ . Four different grid resolutions listed in Table 1 were employed in the simulations. The mesh was unstructured and with a variable cell size, the smallest near the sphere surface to resolve boundary layers, and gradually coarser away from the sphere (Fig. 1).

Table 1: Grid resolution and Strouhal number  $St$

| Mesh         | m0        | m1        | m2         | m3         |
|--------------|-----------|-----------|------------|------------|
| No. of cells | 2,720,848 | 6,085,471 | 11,606,224 | 16,733,944 |
| $St$         | 0.1627    | 0.1750    | 0.1885     | 0.1933     |

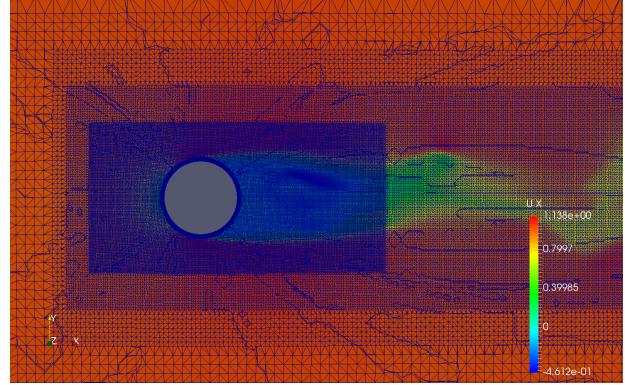


Figure 1: Unstructured mesh

The Navier-Stokes equations were solved using OpenFOAM solver pimpleFoam. The algorithm is based on a blend of transient SIMPLE and PISO algorithms. At each time step, after time  $t$  increases by  $\Delta t$ , the pressure-velocity coupling loop is executed, in which the momentum equation is solved first, followed by a corrector which solves the pressure equation to produce a divergence free velocity field.

At each time step during the simulation all terms in the numerical dissipation equation (5) are computed for an individual finite volume and subsequently integrated over several selected sub-domains. This makes possible to monitor the variation of the numerical dissipation in each sub-domain over entire simulation time. Since there are no periodic boundaries for sub-domains, all terms in (5) are computed by volume integration, which is suitable for the finite volume method used, and gives results consistent with those obtained using surface integration for the flux terms (Castiglioni & Domaradzki, 2015b).

### Strouhal number

The Strouhal number is an important parameter characterizing a weakly turbulent flow past sphere

$$St = \frac{fD}{U}, \quad (8)$$

where  $U$  is the free-stream velocity,  $D$  is the sphere diameter, and  $f$  is the frequency of vortex shedding. In this work we use the Strouhal number as a diagnostic quantity to assess the quality of our simulations by comparison with results of Tomboulides & Orszag (2000) obtained in well resolved spectral DNS. The frequency  $f$  was obtained using FFTs of the streamwise velocity at two locations behind the sphere :  $x = 2.5D, y = 0.3D, z = 0$  and  $x = 5.75D, y = 0.3D, z = 0$ . These are the same locations as in Tomboulides & Orszag (2000), where the most dominant mode was characterized by the Strouhal number  $St_1 = 0.195$ , which we use as the benchmark. Only time series in the statistically steady

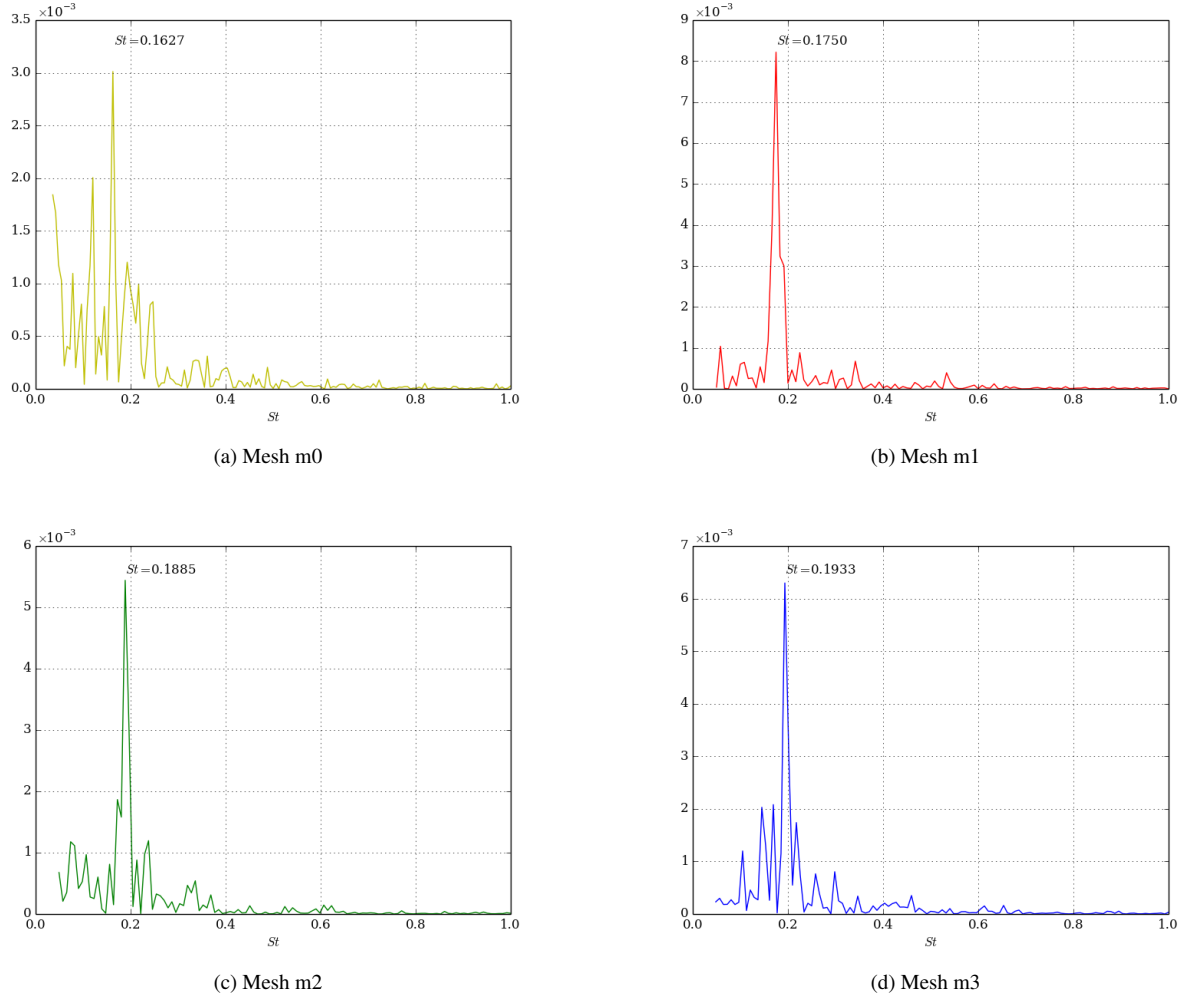


Figure 2: Power spectrum of  $u_x$  (streamwise direction) at  $x = 2.5D, y = 0.3D, z = 0$ .

state ( $t/(D/U) > 50$ ) were used in computing FFTs. Values of the Strouhal number found in the current simulations for all four resolutions are collected in Table 1 and the power spectra are shown in Fig. 2. The values were identical at both locations. The computed Strouhal number changes from  $St = 0.1627$  for the lowest resolution run to  $St = 0.1933$  for the highest resolution run, when satisfactory agreement with the benchmark is reached.

### Numerical Dissipation Analysis

To identify the effects of numerical dissipation rate on the accuracy of simulations and to provide guidance for the mesh refinement five sub-domains, shown in Fig. 3, were selected for the analysis. The number of cells in each sub-domain is given in Table. 2.

Table 2: No. of cells in each sub-domain

| Mesh | m0      | m1      | m2        | m3        |
|------|---------|---------|-----------|-----------|
| r1   | 63,245  | 388,806 | 496,660   | 3,789,930 |
| r2   | 17,974  | 511,797 | 617,889   | 1,002,297 |
| r3   | 69,312  | 529,516 | 554,496   | 554,496   |
| r4   | 335,475 | 556,893 | 1,505,627 | 2,875,146 |
| r5   | 22,216  | 83,573  | 129,812   | 920,560   |

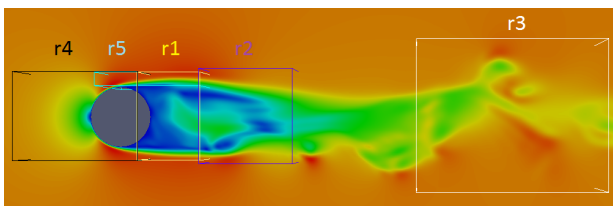
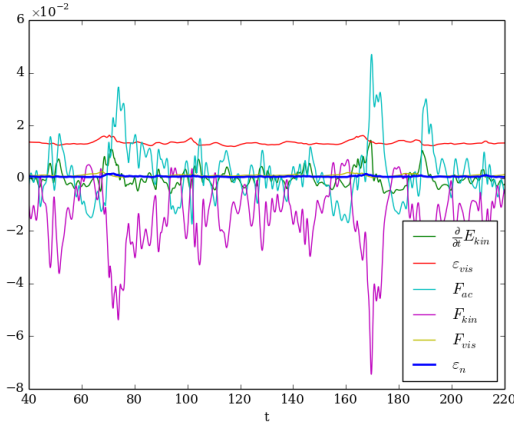
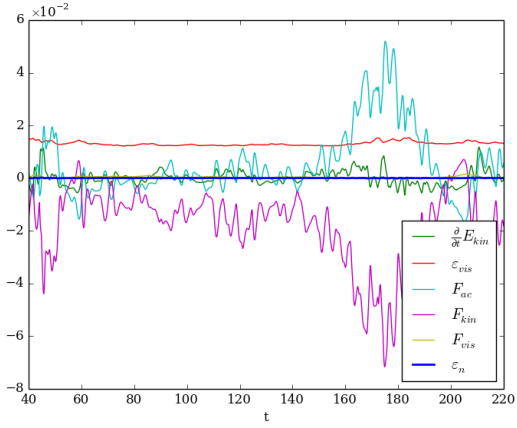


Figure 3: Computational sub-domains

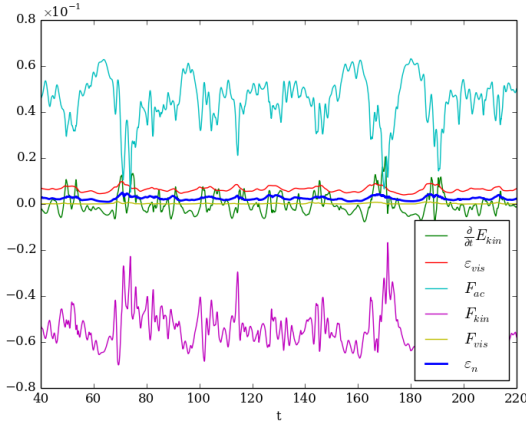
The results for each term in the numerical dissipation equation (5), normalized by the volume of a computational sub-domain, are shown in Fig. 4. Clearly, the numerical dissipation rate is in general quite small compared with the individual terms in the equation (5). However, the numerical dissipation is not negligible and decreases with the increased resolution as shown in Fig. 5. In that figure we plot the ratio of numerical and physical dissipation rate for regions r1, r2, r4 and r5, for all four mesh resolutions, as a function



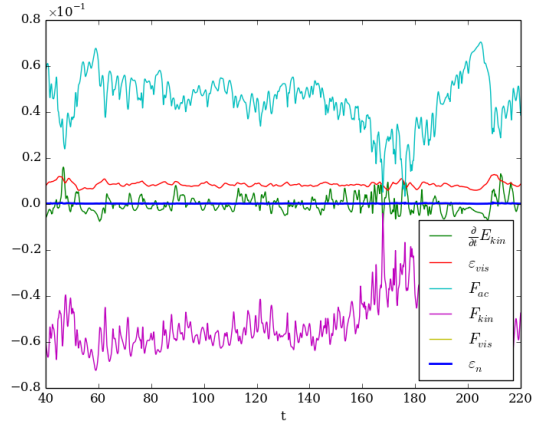
(a) Region r1 coarsest mesh m0



(b) Region r1 finest mesh m3



(c) Region r2 coarsest mesh m0



(d) Region r2 finest mesh m3

Figure 4: Time-evolution of each terms in numerical dissipation equation after volume integration in selected sub-domains. Rate of change of kinetic energy  $\frac{\partial}{\partial t} E_{kin}$  (green line), viscous (or physical) dissipation  $\epsilon_{vis}$  (red line), pressure flux  $F_{ac}$  (cyan line), advective flux  $F_{kin}$  (purple line), viscous flux  $F_{vis}$  (yellow line), and numerical dissipation rate  $\epsilon_n$  (blue line).

of time. The time average values for all cases and sub-domains are also summarized in Table 3. For the coarsest mesh m0, the ratio of the numerical dissipation to the viscous dissipation downstream of the sphere varies from 4 - 5% immediately behind the sphere (sub-domain r1) to 22% further away. For the finest mesh m3, this ratio varies from 0.3% behind the sphere to 6% further away. The large numerical dissipation in the former case is a direct indicator that the simulation results are inaccurate. Indeed, the predicted Strouhal number (Fig. 2(a)) is about 16% lower than the benchmark. Low numerical dissipation in the latter case is an indicator of an acceptable accuracy, with simulation results matching the benchmark (Kim & Durbin, 1988; Tomboulides & Orszag, 2000; Orr *et al.*, 2015). The Strouhal number for intermediate mesh m1 and m2 is 6% and 3% below the benchmark respectively, therefore the numerical dissipation analysis is self-consistent and should provide the correct guidance for mesh refinement.

For turbulent wake flow the physically most significant region is the region right behind the sphere (r1) for which the ratio is reduced from 4.7% to 0.3% between mesh m0 and m3. Focusing on that region (r1), there is a clear correlation between the quality of the prediction for the Strouhal number and the computed numerical dissipation, or rather the ratio of the numerical and the physical

Table 3: Ratio of numerical and physical dissipation (%)

| Regions | m0      | m1     | m2     | m3      |
|---------|---------|--------|--------|---------|
| r1      | 4.6834  | 1.9833 | 0.9699 | 0.3013  |
| r2      | 37.3058 | 5.3602 | 4.3705 | 2.4418  |
| r3      | 22.4156 | 5.8930 | 5.7189 | 6.0572  |
| r4      | 1.9870  | 1.4026 | 0.4342 | -0.6483 |
| r5      | 10.5352 | 7.1840 | 3.2646 | 0.8572  |

dissipation. Since the numerical dissipation rate is an artifact of a discretization of the governing equations it is reasonable to expect that it should be negligible in comparison with the physical, viscous dissipation to get accurate numerical results. Therefore, the ratio of the numerical and physical dissipation in the region behind the sphere is a good indicator of the overall accuracy of a given simulation. The present results demonstrate that this ratio falling

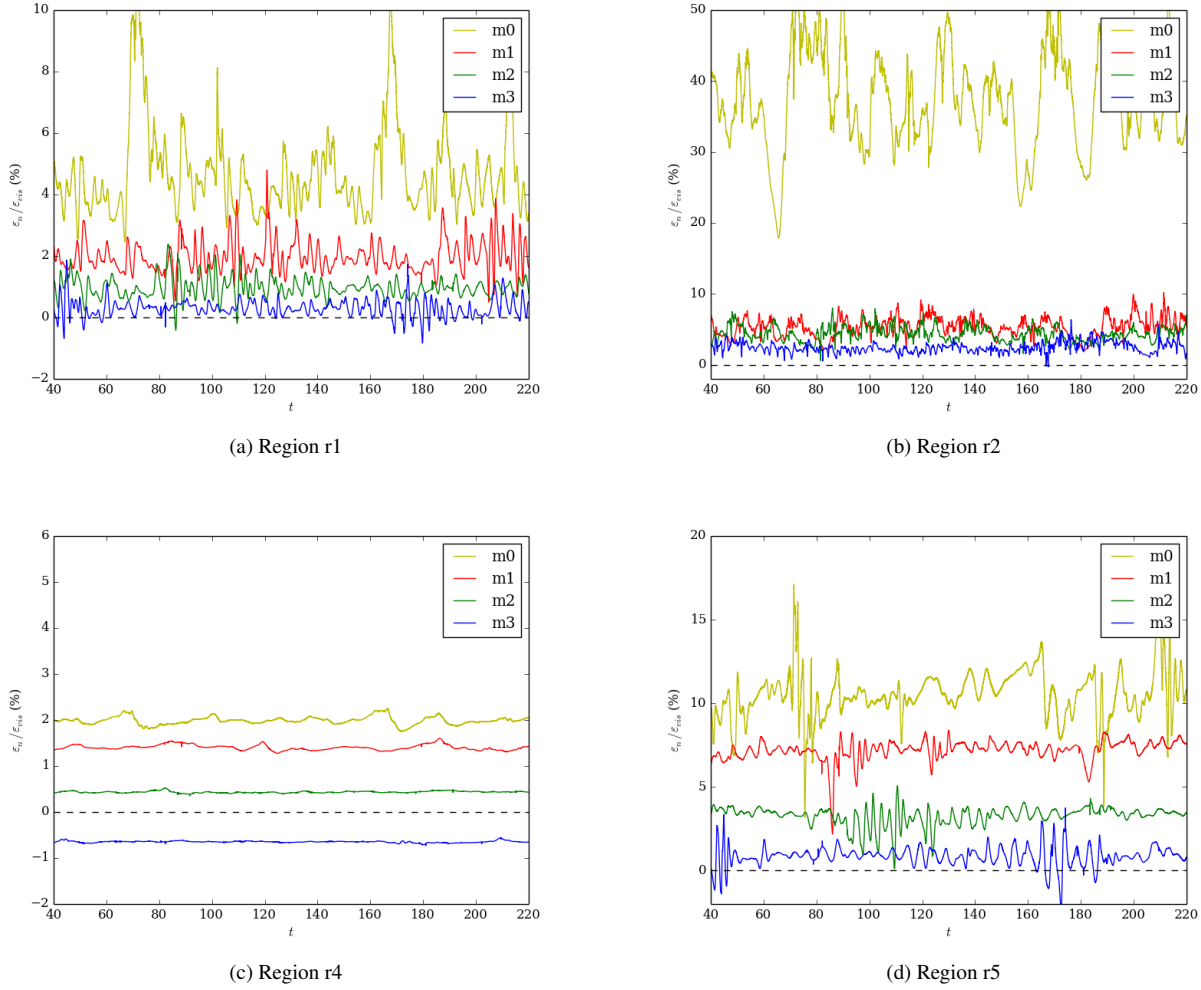


Figure 5: Time-evolution of the ratio of numerical and physical dissipation in selected sub-domains for different grid resolution. Mesh m0 (yellow line), mesh m1 (red line), mesh m2 (green line), mesh m3 (blue line).

below 1% is a good indicator of a numerically accurate DNS.

In fact much smaller ratios of numerical and physical dissipation are difficult to achieve for lower-order schemes and arbitrary unstructured mesh in the present simulations as there may be additional numerical errors when computing derivatives and performing integration over volumes. The effect of mesh refinement is more obvious in the region r2 and r5, where the ratio is very large for mesh m0. On the other hand, the regions of wake far from the sphere (r3) and of the laminar flow before the sphere (r4) are less important for the vortex shedding, therefore, there is no need for further mesh refinement in those regions. In fact, far away from the sphere, the ratio in sub-domain r3 remains almost the same for mesh m1, m2 and m3. Finally, we also selected a small region on the side of the sphere (region r5), considered mainly for grid refinement purpose, where the mesh is curved near the sphere and mesh quality may not be as good as in the other regions. In this way, the refined mesh can be obtained by focusing on only few selected sub-domains and related regions with large numerical dissipation rate.

### Adaptive mesh refinement

In typical DNS applications, the adequate grid resolution in DNS is found through a series of complete runs on successively refined meshes. Based on our analysis of a flow past sphere, the

accuracy of DNS is closely related to the ratio of numerical and physical dissipation in sub-domain r1, right behind the sphere (Fig. 3). Using the same meshes as before (Table 1 and 2), the potential of the numerical dissipation quantification to guide adaptive mesh refinement during simulations, rather than running several simulation through completion, was tested. The refinement and re-mapping was performed using the following stopping criterion:

- Compute the average and maximum value of numerical dissipation ratio in sub-domain r1 over 5 time units. If the average is larger than 1% or maximum value larger than 2%, this indicates that the numerical dissipation is not negligible and thus the grid resolution is inadequate. The simulation should be stopped and the fields re-mapped to a finer mesh using OpenFOAM tool mapFields.

The procedure for the adaptive mesh refinement:

1. Start simulations on the coarsest mesh (m0 in the present case) and run until statistically steady state is reached ( $t = 40$  in the present case).
2. Continue running the simulation for several time units (5 time units in the present case) and invoke the stopping criterion.
3. If it is not satisfied, stop and re-map velocity and pressure fields to a finer mesh generated under the guidance of the numerical

dissipation rate in selected sub-domain(s).

4. Repeat the process as long as the criterion is consistently satisfied in every time unit, which determines the mesh resolution for physically accurate DNS.
5. Continue run for sufficiently long time to obtain required quantities (at least 150 time units to compute the Strouhal number for the current problem).

In Fig. 6 we plot the ratio of the numerical and the physical dissipation obtained in such a process. In Table. 4 the values invoked in the stopping criterion for Region r1 are collected. Looking at the first row the average value drops from 4.147% for mesh m0 to 0.3% for mesh m3. Reaching the physically adequate resolution requires total of 20 time units in the simulation ( $4 \times 5$ ) compared with at least 450 time units required for full simulations on mesh m0, m1, and m2 ( $3 \times 150$ ) before the adequate mesh m3 is found.

Table 4: Stopping criteria for the dissipation ratio (%)

| Mesh    | m0    | m1    | m2    | m3    |
|---------|-------|-------|-------|-------|
| Average | 4.147 | 2.039 | 1.001 | 0.304 |
| Max     | 5.101 | 3.652 | 1.767 | 1.566 |

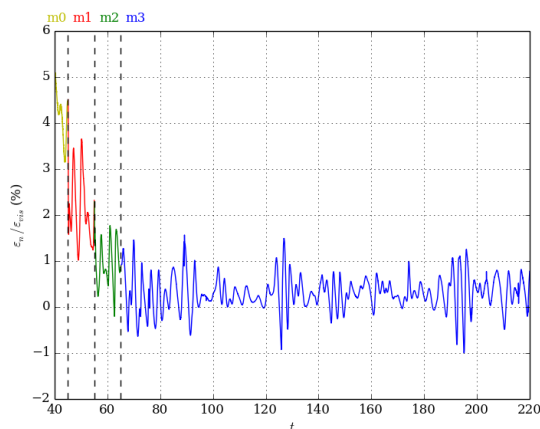


Figure 6: Dissipation ratio for the adaptive mesh refinement in Region r1. Mesh m0 (yellow line), mesh m1 (red line), mesh m2 (green line), mesh m3 (blue line).

## CONCLUSIONS

The numerical dissipation analysis developed by Schraner *et al.* (2015) is applied to a low-order incompressible CFD solver with an unstructured mesh. Simulations of a weakly turbulent wake past a sphere at  $Re = 1000$  show that the numerical dissipation rate directly affects the accuracy of CFD results. Because of that the numerical dissipation can be employed as a convenient tool for estimating the accuracy of simulations in the course of actual runs. Since the numerical dissipation rate is closely related to grid resolution used in selected regions of a computational domain, it can provide a guidance for the adaptive mesh refinement in CFD. It is shown that for the flow problem considered here it is possible to decrease the simulation time needed to reach grid convergence by at least an order of the magnitude. The approach can be easily applied to different CFD solvers and more complex and realistic flow geometries and similar savings in simulation times are expected.

## ACKNOWLEDGEMENTS

This research was supported by NSF grant CBET-1604224. The simulations were performed at the High Performance Computing Center of the University of Southern California.

## REFERENCES

- Castiglioni, G. & Domaradzki, J.A. 2015a A numerical dissipation rate and viscosity in flow simulations with realistic geometry using low-order compressible Navier-Stokes solvers. *Comput. Fluids* **119**, 37–46.
- Castiglioni, G. & Domaradzki, J.A. 2015b On the evaluation of numerical dissipation rate and viscosity in a commercial CFD code. *TSFP-9*.
- Domaradzki, J.A. & Radhakrishnan, S. 2005 Effective eddy viscosities in implicit modeling of decaying high Reynolds number turbulence with and without rotation. *Fluid Dyn. Res.* **36**, 385–406.
- Domaradzki, J.A., Xiao, Z. & Smolarkiewicz, P.K. 2003 Effective eddy viscosities in implicit large eddy simulations of turbulent flows. *Physics of Fluids (1994-present)* **15** (12), 3890–3893.
- Kim, H. J. & Durbin, P. A. 1988 Observations of the frequencies in a sphere wake and of drag increase by acoustic excitation. *Phys. Fluids* **31**, 3260–3265.
- Orr, T. S., Domaradzki, J. A., Spedding, G. R. & Constantinescu, G. S. 2015 Numerical simulations of the near wake of a sphere moving in a steady, horizontal motion through a linearly stratified fluid at  $Re = 1000$ . *Phys. Fluids* **27** (3), 035113.
- Schraner, F. S., Domaradzki, J.A., Hickel, S. & Adams, N. A. 2015 Assessing the numerical dissipation rate and viscosity in numerical simulations of fluid flows. *Comput. Fluids* **114**, 84–97.
- Tomboulides, A. G. & Orszag, S. A. 2000 Numerical investigation of transitional and weak turbulent flow past a sphere. *J. Fluid Mech.* **416**, 45–73.